# TIME-VARYING DELAY ESTIMATION USING COMMON LOCAL ALL-PASS FILTERS WITH APPLICATION TO SURFACE ELECTROMYOGRAPHY

*Christopher Gilliam*[1]*, Adrian Bingham*[1]*, Thierry Blu*[2] *and Beth Jelfs*[1]

[1]School of Engineering, RMIT University, Melbourne, Australia
[2]Department of Electronic Engineering, The Chinese University of Hong Kong

**ABSTRACT**

Estimation of conduction velocity (CV) is an important task in the analysis of surface electromyography (sEMG). The problem can be framed as estimation of a time-varying delay (TVD) between electrode recordings. In this paper we present an algorithm which incorporates information from multiple electrodes into a single TVD estimation. The algorithm uses a common all-pass filter to relate two groups of signals at a local level. We also address a current limitation of CV estimators by providing an automated way of identifying the innervation zone from a set of electrode recordings, thus allowing incorporation of the entire array into the estimation. We validate the algorithm on both synthetic and real sEMG data with results showing the proposed algorithm is both robust and accurate.

***Index Terms***— All-Pass Filters, Surface EMG, Muscle Conductance Velocity, Time-Varying Delay Estimation

## 1. INTRODUCTION

Time dependent delay estimation is a problem that occurs in many areas involving time of flight or speed based measurements. One such problem is the estimation of conduction velocity (CV) from surface electromyography (sEMG). CV describes the speed of propagation of motor unit action potentials (MUAPs) along the muscle fibre and as such is an important factor in the study of muscle activity revealing information regarding pathology, fatigue or pain in the muscle [1]. The estimation of time-varying CV between two or more sEMG signals allows for application to a wider range of conditions and tasks than estimation of a constant CV [2]. The problem of estimating CV from sEMG can be considered in terms of estimating the time-varying delay (TVD) between signals received at spatially separated recording electrodes such that

$$\begin{aligned} g_1(t) &= f(t) + e_1(t) \\ g_2(t) &= f\big(t - \tau(t)\big) + e_2(t) \\ &\vdots \\ g_N(t) &= f\big(t - N\tau(t)\big) + e_N(t), \end{aligned} \tag{1}$$

where $g_n(t)$ is the signal recorded at the $n^{th}$ electrode at time $t$, $N$ is the number of electrodes, $f(t)$ is the signal of interest and $\tau(t)$ is the TVD common to all electrodes. The additive noises $e_n(t)$ are assumed to be i.i.d Gaussian processes.

Delay estimation techniques are classically based upon generalized cross correlation [3] or coherence [4]. A number of approaches to TVD estimation have been proposed [5, 6, 7], however, the issue of estimating TVDs for the purpose of CV estimation is not straightforward. Not all methods perform well in the presence of noise [8] - which can be expected in sEMG and if we want to avoid the need for motor unit decomposition we require a technique which can estimate TVDs with unknown waveforms. There are also a number of factors which can affect the calculation of CV [1] one of the most fundamental of which is the selection of appropriate signals. Currently algorithms require the selection of signals based on either locating the electrode array to avoid the innervation zone (IZ) – MUAPs propagate outwards from the IZ causing a change in sign of the delay (see Section 3.3 for more details) – or selecting a subset of the recorded signals. Many of the existing approaches to the estimation of CV have been based upon the Newton method for aligning waveforms proposed in [9] including extensions to TVD estimation [10]. More recently the use of adaptive filtering [11] and phase based approaches [12] to TVD estimation for CV calculation have been proposed. In [13] a parametric approach was shown to outperform non-parametric approaches. However, this requires appropriate selection of the underlying model and the use of maximum likelihood estimation can be computationally intensive. Therefore, in this paper we present a non-parametric method for the estimation of CV, which is both fast and accurate, and capable of automatically dealing with the change in sign of the delay around the IZ.

The proposed approach is based upon estimating the TVD using local all-pass (LAP) filters. The LAP framework originates in image registration [14] and has previously been used in biomedical [15] and biological [16] imaging. The novelty of our approach is in the adaptation of the framework to allow estimation of a single delay signal that is common to a group of signals as described in (1). More precisely, we propose an algorithm that simultaneously relates local changes across one set of 1D signals to another set using all-pass filters. The algorithm then extracts a per sample estimate of the common TVD from the filters. We term this technique the Common Local All-Pass (CLAP) algorithm. The advantages of this technique are three-fold: first the algorithm can easily and efficiently scale to handle multiple signals. Secondly, due to the nature of CLAP, the IZ can be automatically identified. Finally, once the IZ has been detected, a simple reversal of the order in which some of the signals are processed allows the CLAP to estimate the delay using the whole electrode array. Thus improving the accuracy of the delay estimation by reducing issues surrounding electrode location [17] whilst also avoiding the need for identification of an appropriate signal subset. We demonstrate the accuracy of the proposed approach on both synthetic data and real high density sEMG (HD-sEMG).

## 2. LOCAL ALL-PASS FILTER FRAMEWORK

In this section, we introduce and extend the LAP framework presented in [14, 18] to TVD estimation.

Email: dr.christopher.gilliam@ieee.org

### 2.1. Concept 1 - A constant delay is all-pass filtering

The first element of the framework is the concept that a constant delay, $\tau$, is equivalent to all-pass filtering. This concept follows from the Fourier shift theorem

$$x_2(t+\tau) = x_1(t) \iff X_2(\omega) = X_1(\omega)\,\mathrm{e}^{-j\tau\omega}, \quad (2)$$

where $x$ is a generic signal, $X$ represents its Fourier transform and $\omega$ denotes the frequency coordinate. Thus, if we define a filter $h$ with a frequency response $H(\omega) = \mathrm{e}^{-j\tau\omega}$ then $x_2$ is a filtered version of $x_1$ and the filter, $h$, is all-pass in nature. Accordingly, estimating the filter $h$ is a proxy for determining the delay in (2).

### 2.2. Concept 2 - Linearising the all-pass constraint

The next concept is that the $2\pi$-periodic frequency response $H(\omega)$ of any digital all-pass filter can always be expressed as

$$H(\omega) = \frac{P\left(\mathrm{e}^{j\omega}\right)}{P\left(\mathrm{e}^{-j\omega}\right)}, \quad (3)$$

where $P\left(\mathrm{e}^{j\omega}\right)$ is the forward and $P\left(\mathrm{e}^{-j\omega}\right)$ the backward version of a real digital filter $p$. Using the above expression, the all-pass filtering operation performed by $h$ can be expressed linearly as a function of $p$

$$x_2[k] = h[k] * x_1[k] \iff p[-k] * x_2[k] = p[k] * x_1[k], \quad (4)$$

where $*$ is the convolution operator and $k$ denotes discrete time. Thus, estimating $p$ is equivalent to determining the all-pass filter $h$.

### 2.3. Concept 3 - Basis representation of the all-pass filter

The final concept is to approximate $p$ using a linear combination of a few fixed, known, real filters $p_n$, i.e.

$$p_{\text{app}}[k] = \sum_{l=0}^{L-1} c_l p_l[k], \quad (5)$$

where $L$ denotes the number of filters and $c_l$ are the coefficients. The advantage of such an approximation is that the estimation of $h$ is further reduced to determining the $L$ coefficients $c_l$.

A simple choice of filter basis would be the canonical representation of an finite impulse response (FIR) filter with a support $k \in [-R, R]$, thus $L = 2R + 1$. However, limiting the support of the filter $p_{\text{app}}$ will limit the size of the delay to a maximum of $R$ samples. Therefore, the canonical basis quickly becomes too expensive when estimating large delays as $N \propto R$. Instead, [14, 18] proposed a compact, scalable, basis that spans the derivatives of a Gaussian function. For this paper, we use the Gaussian function and its first derivative as the filter basis thus $L = 2$. These filters are defined as

$$p_0[k] = \mathrm{e}^{-k^2/2\sigma^2} \quad \text{and} \quad p_1[k] = k p_1[k], \quad (6)$$

where $\sigma = R/2 - 0.2$ and $R$ is the integer half support of the filters. For a theoretical foundation for such a basis we refer readers to the analysis presented in [19].

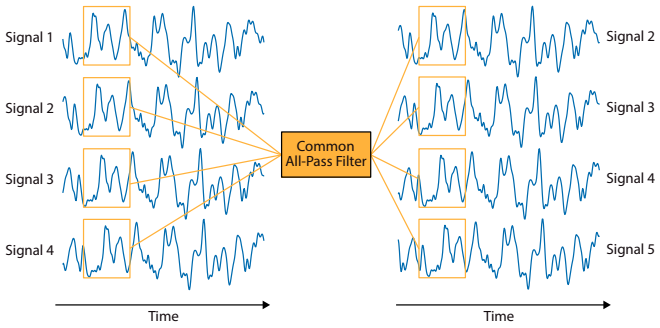


**Fig. 1**. Diagram illustrating the principle of the CLAP algorithm. Local regions on the left-hand side are related to corresponding locations on the right-hand side via a common all-pass filter.

### 2.4. Local All-Pass (LAP) Algorithm

Using the above concepts, the LAP algorithm functions by assuming the TVD, $\tau(t)$, is approximately constant within a local window $\mathcal{W}$ and estimating an all-pass filter for that window using (4) and (5). This process is then repeated by shifting the window $\mathcal{W}$ and estimating a new all-pass filter. The final result is that the LAP estimates a local all-pass filter per sample (a filter corresponds to the central sample in $\mathcal{W}$). A filter is estimated by solving

$$\min_{c_1} \sum_{k \in \mathcal{W}} \left| p_{\text{app}}[k] * x_1[k] - p_{\text{app}}[-k] * x_2[k] \right|^2, \quad (7)$$

where $p_{\text{app}}[k] = p_0[k] + c_1 p_1[k]$. Importantly, as we set $c_0 = 1$, this minimisation is equivalent to solving a linear system of equations with 1 unknown, which can be implemented very efficiently using convolution and pointwise multiplication [14, 18].

The final stage of the LAP is to extract the estimate of the TVD from the local all-pass filters. Using the all-pass structure, the delay estimate from a single all-pass filter can be expressed in term of the the impulse response of $p_{\text{app}}$

$$\hat{\tau} = 2\frac{\sum_k k p_{\text{app}}[k]}{\sum_k p_{\text{app}}[k]}. \quad (8)$$

## 3. ESTIMATING A COMMON TIME-VARYING DELAY

We now consider the estimation of a TVD that is common across a set of signals and present the Common Local All-Pass (CLAP) algorithm.

### 3.1. Common Local All-Pass Filters

The ensemble of signals described in (1) are characterised by the same TVD $\tau(t)$. Thus, rather than running the LAP on each adjacent pair of signals, we propose estimating one common delay from the whole ensemble of signals. Specifically, our goal is to relate a local region across a subset of the ensemble to the corresponding region across another subset of signals using a common all-pass filter. An illustration of this common all-pass filter is shown in Fig. 1. Given an ensemble of signals $x_n(t), n = 1, 2, \ldots, N$, we adapt the local minimisation in (7) as follows

$$\min_{c_1} \sum_{n=1}^{N-1} \sum_{k \in \mathcal{W}} \left| p_{\text{app}}[k] * x_n[k] - p_{\text{app}}[-k] * x_{n+1}[k] \right|^2, \quad (9)$$

where $p_{\text{app}}[k] = p_0[k] + c_1 p_1[k]$. The estimate of the common delay is then obtained using (8).

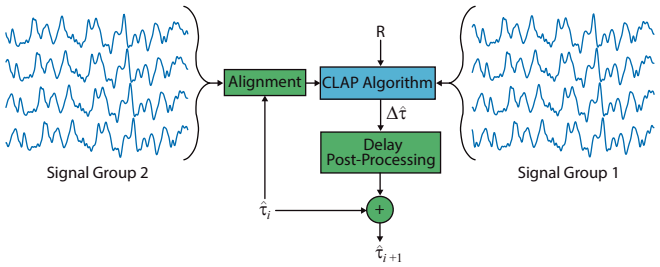


**Fig. 2**. Diagram illustrating the multi-scale framework for the CLAP. Note that $R$ is the half-support of the CLAP filters, $\hat{\tau}_i$ is the estimate of the delay at the $i$th iteration and $\Delta\hat{\tau}$ is the delay increment obtained from the CLAP.

### 3.2. Multi-Scale Framework

Although the CLAP is capable of estimating large delays, it requires a filter basis with a large support to do so - the half support of the filters, $R$, is the upper bound on the size of the delay that can be estimated. This is equivalent to assuming large regions of the delay signal are slowly varying. Accordingly, we use an iterative multi-scale framework to estimate both fast and slow varying delays. In brief, large values of $R$ are used to estimate the large slowly varying parts of the delay, then smaller values of $R$ are used for smaller faster variation in the delay. A diagram of this multi-scale framework is shown in Fig. 2. The framework also includes the following processing steps: i) Alignment - a procedure whereby the second set of signals is warped closer to the first set using the current estimate of the TVD. This alignment is achieved using high quality interpolation [20, 21]. ii) Delay Post-Processing - this step comprises two elements: Firstly, an inpainting procedure [22] to replace erroneous delay estimates caused if (9) is singular. These estimates are identified if their size is larger than the current value of $R$. Secondly, Gaussian filtering is performed to smooth any errors not previously identified.

### 3.3. Application to sEMG

For application to sEMG signals we require two further processing steps. The first step is to use the single differential of the signals rather than the raw recordings, i.e. $x_n(t) = g_{n+1}(t) - g_n(t)$, as sEMG recordings are likely to suffer a common source of corruption across all of the channels. The second step is to identify the IZ. The IZ occurs at the point where motor neurons innervate the muscle fibres, at this point the MUAPs propagate outwards towards the tendons. Typically, to allow calculation of the CV, either the location of the IZ is identified prior to the recording and the electrode array placed to one side - which is not always practical - or the signals are visually inspected to identify the IZ - which due to the small size of the delay is not always clear - and a subset of the signals selected.

Instead, we run the normal LAP algorithm across each pair of adjacent signals and calculate the mean value of the delay between the signals. Using these values, the IZ is identified as the point where the sign of the mean delays switches. Given this switching point, the order in which we process the signals above the zone is reversed. This switches the sign of the corresponding delays so they are consistent with the signals below the IZ and can be processed all together using the CLAP algorithm.

## 4. DATA

### 4.1. Synthetic Data Model

The synthetic data was simulated based on a model which has previously been used to test CV estimation algorithms [2, 13]. The

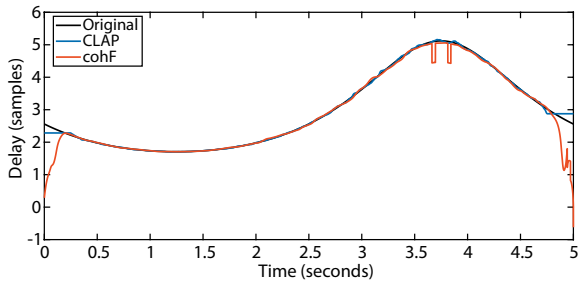


(a) Noiseless Data

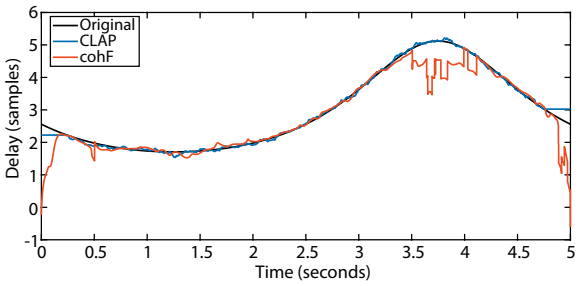


(b) SNR=10dB

**Fig. 3**. Example delay estimates obtained from 6 signals.

first channel is obtained by filtering white Gaussian noise through a FIR from a known spectrum with EMG like properties [23]. Subsequent channels are then obtained by interpolating the previous channel with the delay $\tau(t)$. The delay can be related to the CV by $\tau(t) = F_s \frac{\Delta e}{CV(t)}$, where the sampling frequency $F_s = 2048$Hz and the inter electrode distance $\Delta e = 5$mm. The CV is defined as $CV = 4 + 2\sin(2\pi 0.2t/F_s)$ resulting in biologically plausible ranges from 2m/s to 6m/s with maximum acceleration of 2.51m/s$^2$. To further simulate experimental data, the synthetic signals are corrupted by additive white Gaussian noise and then low-pass filtered to simulate the response of the sEMG acquisition device.

### 4.2. Experimental Data

HD-sEMG was recorded from 3 male participants, all participants provided informed consent and the experimental protocol was approved by the Human Research Ethics Committee, RMIT University. The HD-sEMG electrodes were arranged in a $4 \times 16$ array with 5mm inter electrode distance and sampling rate of 2441Hz. The array was placed such that the columns were oriented close to parallel with the muscle fibres of the biceps brachii with reference electrodes placed on the elbow. Participants were seated on a chair with their dominate arm resting on an table. In this position the participants were asked to pull on a fixed cable attached to a force sensor. Prior to the experiment the participant's maximum voluntary contraction (MVC) was recorded. The participant was then asked to maintain a contraction at 40% of their MVC until they had reached task failure or they felt pain. The real time output of the force sensor and the required force were displayed to the participant. After completing the 40% MVC contraction the participant waited 30 minutes to reduce any effects of muscle fatigue and then repeated the experiment for 80% MVC.

### 4.3. Surrogate Data

As the true CV of the experimental data is unknown, we use a surrogate data method [24, 25] to validate the legitimacy of the results obtained from the CLAP. The surrogate data was generated using an

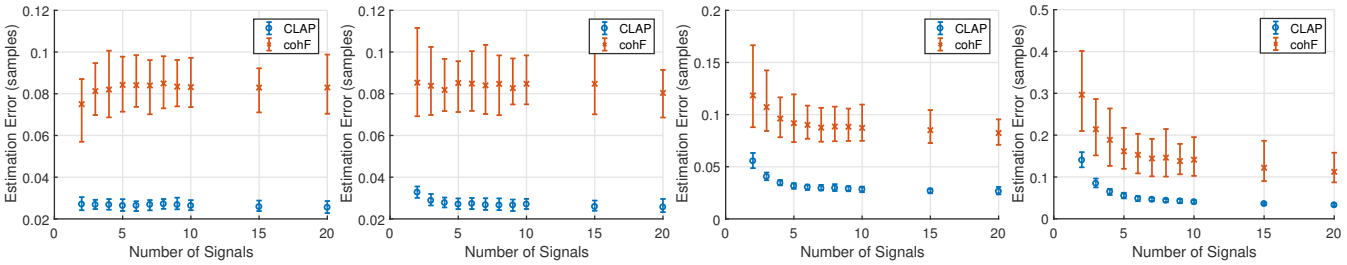


(a) Noiseless Data (b) SNR=30dB (c) SNR=20dB (d) SNR=10dB

**Fig. 4**. Average errors in delay estimates for increasing signal numbers. Error bars indicate $5^{\text{th}}$ and $95^{\text{th}}$ quantiles.

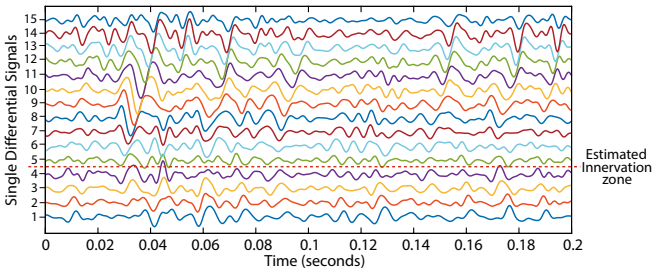


**Fig. 5**. Example single differential signals with location of the innervation zone indicated.

iterative amplitude adjusted FFT to preserve both the amplitude and frequency distributions of the data whilst destroying any time dependencies [26]. For each pair of signals used to estimate the delay one was left unaltered and surrogates of the other created. This process was repeated 100 times to obtain a statistical average.

## 5. RESULTS

### 5.1. Synthetic Data Results

To test the accuracy of the proposed approach 100 different realisations were produced for noiseless and SNR = 30, 20 and 10dB scenarios with varying number of simulated signals. The results obtained were compared against the Fourier phase coherency (CohF) as it has previously been shown to have better performance in the presence of noise than alternative algorithms [2]. Figure 3 shows illustrative examples of the estimates of the true delay obtained with the CLAP and CohF algorithms for 6 signals in both the noiseless and SNR=10dB cases. The window size of the algorithms were set to 512 samples (equivalent to 0.25s). As can be seen even in the noiseless case the CohF algorithm does not perform well when the acceleration is larger, whereas the CLAP due to its multi-scale nature can accurately estimate both slow and fast changing delays. The average errors in the delay estimates for both algorithms are shown in Fig. 4. The figure highlights that the CLAP outperforms CohF in terms of both accuracy and robustness for all scenarios.

### 5.2. Experimental Data Results

Initially for each column of the electrode array the method from Section 3.3 was used to estimate the location of the IZ. Figure 5 shows example single differential signals and the estimated location of the IZ. Based upon this location the order of the pairs of signals with negative delay estimates were switched allowing estimation of a single common delay from all signals.

Table 1 provides a summary of the estimates of the TVDs obtained from both the real data and the average of 100 surrogates.

**Table 1**. Comparison of the delays estimated from the experimental and surrogate data. $\bar{\tau}$ is the time averaged delay and $\beta$ the slope of the regression.

| Subject | MVC | Data | | Surrogates | | |
|---|---|---|---|---|---|---|
| | | $\bar{\tau}$ | $\beta$ $(\times 10^{-3})$ | Avg $\bar{\tau}$ | Var $\bar{\tau}$ | Avg $\beta$ $(\times 10^{-3})$ |
| 1 | 40% | 2.503 | 0.7 | -0.001 | 0.000 | -0.0 |
| | 80% | 2.363 | 13.5 | -0.003 | 0.000 | 0.1 |
| 2 | 40% | 2.320 | 2.2 | -0.001 | 0.000 | -0.1 |
| | 80% | 2.399 | 8.3 | 0.000 | 0.002 | 0.5 |
| 3 | 40% | 1.690 | 0.2 | 0.001 | 0.000 | -0.0 |
| | 80% | 1.726 | 4.0 | -0.002 | 0.001 | 0.1 |

The table shows there is a clear distinction between the two sets of results; without any time structure the average of the mean delay is close to zero with a variance in the estimates of the mean delay also close to zero. This is not the case with the real data indicating the delays originate in the data rather than from bias in the estimator. Furthermore the time average of the delays from the real data relate to mean CVs of 4.89m/s, 5.20m/s, 5.28m/s, 5.11m/s, 7.26m/s and 7.13m/s all of which fall within recommended constraints of 2-8m/s [13].

To compare the time-varying properties of the data linear regression of the delay estimates was performed, the slope of the regressions are presented in Table 1. From these results it can be seen that for all three subjects the 80% MVC delay estimates have slopes that indicate an increase in delay corresponding to decreasing CVs of $-0.0287$, $-0.0174$ and $-0.0168$ which are in line with previously observed results which indicate a decrease in CV with fatigue [10].

## 6. CONCLUSIONS

In this paper, we have presented an algorithm for estimating a common TVD from an ensemble of signals and applied it to the problem of determining CV from sEMG. Our algorithm is based on using a common all-pass filter to relate local changes in one group of signals to changes in another group. We demonstrated that this algorithm is more accurate and robust than standard approaches used in CV estimation under synthetic conditions. Finally, we presented initial results for CV estimation on real datasets. The estimated TVDs provided biologically plausible CV values while at the same time validation via surrogate testing indicated that the delays obtained occurred due to structure in the data. Currently, we are investigating combining our approach with the parametric iterative fitting outlined in [27].

## 7. REFERENCES


[1] D. Farina and R. Merletti, "Methods for estimating muscle fibre conduction velocity from surface electromyographic signals," *Med. Biol. Eng. Comput.*, vol. 42, no. 4, pp. 432–445, 2004.

[2] P. Ravier, D. Farina, and Buttelli O., "Time-varying delay estimators for measuring muscle fiber conduction velocity from the surface electromyogram," *Biomed. Signal Process. Control*, vol. 22, pp. 126–134, 2015.

[3] C. Knapp and G. Carter, "The generalized correlation method for estimation of time delay," *IEEE Trans. Acoust., Signal Process.*, vol. 24, no. 4, pp. 320–327, 1976.

[4] G. C. Carter, "Coherence and time delay estimation," *Proc. IEEE*, vol. 75, no. 2, pp. 236–255, 1987.

[5] D. Etter and S. Stearns, "Adaptive estimation of time delays in sampled data systems," *IEEE Trans. Acoust., Signal Process.*, vol. 29, no. 3, pp. 582–587, 1981.

[6] Y. Chan, J. Riley, and J. Plant, "Modeling of time delay and its application to estimation of nonstationary delays," *IEEE Trans. Acoust., Signal Process.*, vol. 29, no. 3, pp. 577–581, 1981.

[7] I. M. G. Lourtie and J. M. F. Moura, "Optimal estimation of time-varying delay," in *Proc. Int. Conf. Acoust., Speech, and Signal Process., (ICASSP)*, New York, NY, USA, 1988, pp. 2622–2625.

[8] H. C. So, "Comparison of DDE and ETDGE for time-varying delay estimation," *Electron. Lett.*, vol. 35, no. 23, pp. 1994, 1999.

[9] K. C. McGill and L. J. Dorfman, "High-resolution alignment of sampled waveforms," *IEEE Trans. Biomed. Eng.*, vol. BME-31, no. 6, pp. 462–468, 1984.

[10] D. Farina, M. Pozzo, E. Merlo, A. Bottin, and R. Merletti, "Assessment of average muscle fiber conduction velocity from surface EMG signals during fatiguing dynamic contractions," *IEEE Trans. Biomed. Eng.*, vol. 51, no. 8, pp. 1383–1393, 2004.

[11] F. Leclerc, P. Ravier, D. Farina, J.-C. Jouanin, and Buttelli O., "Time-varying delay estimation with application to electromyography," in *Proc. European Signal Process. Conf. (EUSIPCO)*, Lausanne, Switzerland, 2008.

[12] F. Leclerc, P. Ravier, O. Buttelli, and J.-C. Jouanin, "Comparison of three time-varying delay estimators with application to electromyography," in *Proc. European Signal Process. Conf. (EUSIPCO)*, Poznan, Poland, 2007.

[13] A. Boualem, M. Jabloun, P. Ravier, and O. Buttelli, "Legendre polynomial modeling of time-varying delay applied to surface EMG signals—derivation of the appropriate time-dependent CRBs," *Signal Process.*, vol. 114, pp. 34–44, 2015.

[14] C. Gilliam and T. Blu, "Local all-pass geometric deformations," *IEEE Trans. Image Process.*, vol. 27, no. 2, pp. 1010–1025, 2018.

[15] C. Gilliam, T. Küstner, and T. Blu, "3D motion flow estimation using local all-pass filters," in *Proc. IEEE Int. Symp. Biomed. Imag. (ISBI)*, Prague, Czech Republic, 2016, pp. 282–285.

[16] J. Li, C. Gilliam, and T. Blu, "A multi-frame optical flow spot tracker," in *Proc. IEEE Int. Conf. Image Process. (ICIP)*, Québec City, Canada, 2015, pp. 3670–3674.

[17] D. Farina and R. Merletti, "Estimation of average muscle fiber conduction velocity from two-dimensional surface EMG recordings," *J. Neurosci. Methods*, vol. 134, no. 2, pp. 199–208, 2004.

[18] C. Gilliam and T. Blu, "Local all-pass filters for optical flow estimation," in *Proc. IEEE Int. Conf. Acoust. Speech Signal Process. (ICASSP)*, Brisbane, Australia, 2015, pp. 1533–1537.

[19] T. Blu, P. Moulin, and C. Gilliam, "Approximation order of the LAP optical flow algorithm," in *Proc. IEEE Int. Conf. Image Process. (ICIP)*, Québec City, Canada, 2015, pp. 48–52.

[20] P. Thévenaz, T. Blu, and M. Unser, "Interpolation revisited," *IEEE Trans. Med. Imag.*, vol. 19, no. 7, pp. 739–758, 2000.

[21] T. Blu, P. Thévenaz, and M. Unser, "MOMS: Maximal-order interpolation of minimal support," *IEEE Trans. Image Process.*, vol. 10, no. 7, pp. 1069–1080, 2001.

[22] M. Oliveira, B. Bowen, and R. McKenna *et al.*, "Fast digital image inpainting," in *Proc. Int. Conf. Visual. Imag. Image Process. (VIIP)*, Marbella, Spain, 2001, pp. 261–266.

[23] E. Shwedyk, R. Balasubramanian, and R. N. Scott, "A nonstationary model for the electromyogram," *IEEE Trans. Biomed. Eng.*, vol. BME-24, no. 5, pp. 417–424, 1977.

[24] J. Theiler, S. Eubank, A. Longtin, B. Galdrikian, and J. D. Farmer, "Testing for nonlinearity in time series: the method of surrogate data," *Physica D*, vol. 58, no. 1-4, pp. 77–94, 1992.

[25] T. Schreiber and A. Schmitz, "Surrogate time series," *Physica D*, vol. 142, no. 3-4, pp. 346–382, 2000.

[26] T. Schreiber and A. Schmitz, "Improved surrogate data for nonlinearity tests," *Phys. Rev. Lett.*, vol. 77, no. 4, pp. 635–638, 1996.

[27] X. Zhang, C. Gilliam, and T. Blu, "Iterative fitting after elastic registration: An efficient strategy for accurate estimation of parametric deformations," in *Proc. IEEE Conf. Image Processing (ICIP)*, Beijing, China, 2017, pp. 1492–1496.